Biogeosciences Discuss., 12, 17781–17816, 2015
www.biogeosciences-discuss.net/12/17781/2015/
doi:10.5194/bgd-12-17781-2015

Biogeosciences Discussions
Open Access
EGU

The significance of nitrogen regeneration for new production within a filament of the Mauritanian upwelling system

D. R. Clark, C. E. Widdicombe, A. P. Rees, and E. M. S. Woodward

Plymouth Marine Laboratory, Prospect Place, West Hoe, Plymouth, PL1 3DH, UK

Received: 23 October 2015 – Accepted: 26 October 2015 – Published: 6 November 2015

Correspondence to: D. R. Clark (drcl@pml.ac.uk)

Published by Copernicus Publications on behalf of the European Geosciences Union.

Abstract

The lagrangian progression of biogeochemical processes was followed in a filament of the Mauritanian upwelling system, North West Africa, during offshore advection. Inert duel tracers sulphur hexafluoride and helium-3 labelled a freshly upwelled patch of water that was mapped for 8 days. Changes in biological, physical and chemical characteristics were measured including phytoplankton productivity, nitrogen assimilation and regeneration. Freshly upwelled water contained high nutrient concentrations ($NO_3^- = 9.0 \pm 0.1\,\mu mol\,L^{-1}$; $PO_4^{3-} = 0.7 \pm 0.1\,\mu mol\,L^{-1}$; $Si = 2.7 \pm 0.1\,\mu mol\,L^{-1}$) but was depleted in N compared to Redfield stoichiometry (N : P = 13.9 : 1). A maximum primary productivity rate of $0.7\,mol\,C\,m^{-2}\,d^{-1}$ was measured on the continental shelf, associated with N-assimilation rates of $43.8\,nmol\,L^{-1}\,h^{-1}$ for NO_3^-, $32.8\,nmol\,L^{-1}\,h^{-1}$ for NH_4^+ and a phytoplankton community dominated by diatoms and flagellates. Indicators of phytoplankton abundance and activity decreased as the labelled water mass transited the continental shelf slope into deeper water, possibly linked to the mixed layer depth exceeding the light penetration depth. By the end of the study, primary productivity rates of $0.1\,mol\,C\,m^{-2}\,d^{-1}$ were measured, associated with N-assimilation rates of $3.9\,nmol\,L^{-1}\,h^{-1}$ for NO_3^-, $6.1\,nmol\,L^{-1}\,h^{-1}$ for NH_4^+ and lower nutrient concentrations ($NO_3^- = 4.6 \pm 0.3\,\mu mol\,L^{-1}$; $PO_4^{3-} = 0.4 \pm 0.1\,\mu mol\,L^{-1}$; $Si = 0.9 \pm 0.1\,\mu mol\,L^{-1}$). Nitrogen regeneration and assimilation took place simultaneously; NH_4^+ was regenerated at 9.4–85.0 $nmol\,L^{-1}\,h^{-1}$; NH_4^+ was oxidised at 0.30–8.75 $nmol\,L^{-1}\,h^{-1}$; NO_2^- was oxidised at 25.55–81.11 $nmol\,L^{-1}\,h^{-1}$. Results highlight the importance of regenerated NH_4^+ in sustaining phytoplankton productivity and indicate that the upwelled NO_3^- pool contained an increasing fraction of regenerated NO_3^- as it advected offshore. By calculating this fraction and incorporating it into an *f* ratio formulation we estimated that of the 12.38 Tg C of annual regional production, 4.73 Tg C was exportable.

BGD
12, 17781–17816, 2015

1 Introduction

The combination of northeast trade winds and the Coriolis effect due to earth's rotation drives the upwelling of deep nutrient-rich waters into the photic zone of coastal regions in eastern ocean boundaries. Upwelling supports characteristically enhanced biological production and valuable ecosystem services typified by fisheries (Pauly and Christensen, 1995; Arístegui et al., 2009). The maturation and development of biological communities within upwelled water masses as they advect offshore reflects a characteristic feature of eastern boundary upwelling ecosystems (EBUE); the spatial separation of nutrient sources and sinks. Gauging the extent of biological production ultimately exported from upwelling regions is an area of continuing investigation and model development (Álvarez-Salgado et al., 2007; Arístegui et al., 2009).

The North West African upwelling system is possibly the least studied of the four global EBUE's (California, Peru–Chile, Iberia/NW Africa, Benguela) and is potentially the most complex due to its topography and circulation (Mittelstaedt, 1991; Tomczak and Godfrey, 2003; Arístegui et al., 2006; Chavez and Messié, 2009; Meunier et al., 2012). The Mauritanian region within this system is characterised by a relatively wide shelf area over which upwelled water influences biological productivity (Mittelstaedt, 1991), while extended filaments and island induced eddies are additional features (Arístegui et al., 2009). The system can be separated into two regimes; the region between 15 and 20° N undergoes periodic upwelling which dominates during winter and spring, whereas the region north of 20° N is characterised by year round coastal upwelling with maximum intensity during summer and autumn (Mittelstaedt, 1991). The study region, located between 20–22° N, lies at the confluence between the two source waters upwelled in this system (North Atlantic Central Water and South Atlantic Central Water; Mittelstaedt, 1991), which differ in their salinity, temperature and nutrient characteristics. Nutrient concentrations and potential rates of new production in this region are towards the upper limits of the range reported for global EBUEs (Chavez and Messié, 2009).

BGD
12, 17781–17816, 2015

The highly dynamic nature of upwelling systems challenges our ability to understand how biological activity develops as water masses advect offshore. Both eulerian (occupying a fixed location over time through which upwelled water passes) and lagrangian (occupying a water mass as it passes through space and time) strategies have been adopted. The eulerian approach was successfully applied in a study of the Northern Benguela by Postel et al. (2014); a challenge facing this approach is the risk that stations do not sample successive changes in upwelled water due to the dynamic meandering nature of advective transport. Drifting buoys have been used in previous lagrangian studies of upwelling regions (Joint et al., 2001; Wilkerson and Dugdale, 1987) although buoy tracks diverge over time (D'Asaro, 2004) leading to uncertainty about the location of upwelled water masses. To address some of these issues, the inert gases sulphur hexafluoride (SF_6) and helium-3 (^3He) were used to label a water body within a recently upwelled filament. In combination with drifting buoys and mapping exercises, the progression of this labelled water mass and its associated biological activity was followed in lagrangian mode during offshore advection. Our objective was to investigate phytoplankton productivity, microbial nitrogen cycling and to estimate exportable new production.

The assimilation of nitrogen by phytoplankton was introduced as a means of estimating "new" and "exportable" production (*f* ratio; Dugdale and Goering, 1967; Eppley and Peterson, 1979), based on the assumption that NO_3^- regeneration and assimilation processes were spatially distinct, being associated with the aphotic and photic zones respectively. Consequently, the physical introduction of NO_3^- to the photic zone was deemed capable of supporting an increase in phytoplankton productivity. All other forms of nitrogen were deemed to be regenerated (e.g. NH_4^+), having previously been subject to microbial activity and capable only of sustaining rather than enhancing phytoplankton growth. According to this concept, upwelling regions, which characteristically introduced deep nutrient rich waters to the photic zone, were associated with high *f* ratios (i.e. > 0.7) reflecting the high proportion of total N-assimilation supported by NO_3^-. By contrast, strong stratification supressed nutrient inputs to the photic zone of olig-

BGD
12, 17781–17816, 2015

otrophic gyres and biological competition for limited nutrient resources maintained very low NO_3^- concentrations and f ratios (i.e. < 0.1). Investigators have offered tractable means of addressing limitations associated with this concept since its introduction, such as the influence of isotope dilution due to nitrogen regeneration (Glibert et al., 1982; Kanda et al., 1987). However, the assumption that NO_3^- is not regenerated within the photic zone is now known to be inaccurate (Ward, 2008). This last point perhaps presents the greatest challenge to the utility of the new production paradigm. While the simultaneous assimilation and regeneration of NO_3^- can be measured (Fernández et al., 2005, 2009; Benavides et al., 2014; Clark et al., 2014) and potentially accounted for (Fernández and Raimbault, 2007), the fraction of previously regenerated NO_3^- cannot be estimated readily (Martin and Pondaven, 2006). Consequently, the fraction of photic zone NO_3^- that is actually representative of "new" NO_3^- is uncertain. Upwelling areas are an exception; seawater upwelled in the Mauritanian upwelling system may be regarded as genuinely "new" to the photic zone, consistent with the original concept. Here we aimed to address the significance of nitrification for new production estimates in the Mauritanian Upwelling system.

2 Materials and methods

The study was undertaken on board the RRS Discovery (D338; 15 April to 27 May 2009) as a UK contribution to the international Surface Ocean Lower Atmosphere Study (SOLAS) project. Remotely sensed sea surface temperature and chlorophyll *a* data was used to identify a region of active upwelling. Surveys of water column physical structure were conducted in order to select the position for drifter buoy deployment. $SF_6/^3He$ was deployed in a patch (hereafter referred to as P_1) at a depth of 5 m around the drifter (Nightingale et al., 2000). Daily surveys for $SF_6/^3He$ using on-board GC detection ensured that seawater sampling was centred upon the labelled water mass and that the same water mass was sampled until tracer concentrations

BGD
12, 17781–17816, 2015

could no longer be detected reliably. Chemical, physical and biological characteristics of the water mass were measured during the lagrangian study.

Seawater samples were collected from CTD rosette-mounted Niskin bottles which sampled routinely at a depth equivalent to 55 % of surface photosynthetically active radiation (sPAR). Where water column depth permitted, samples were collected less frequently at 1 % sPAR. The assimilation and regeneration of DIN was investigated using ^{15}N amended seawater during deck incubations (Clark et al., 2014). Simultaneously, size fractionated primary productivity was measured in depth profiles using deck incubations with ^{14}C (Tilstone et al., 2009). For all deck incubations, neutral density filters simulated sPAR according to Joint Global Ocean Flux Study protocols (Intergovernmental Oceanographic Commission, 1994) and temperature control was achieved by flushing boxes with seawater from the ships sea-surface supply collected at ≈ 5 m.

2.1 Nitrogen regeneration investigations

A 24-position stainless steel rosette system was used to collect seawater from specific depths using 20 L Niskin bottles. Water columns were characterised during casts using additional instrumentation attached to the rosette, which included Seabird 9 Plus conductivity, temperature, depth (CTD) units, a Seabird SBE 43 dissolved oxygen sensor and a Chelsea MKIII Aquatracka fluorometer. Seawater was collected during pre-dawn casts (approximately 04:00 GMT) at depths equivalent to specific sPAR values, which were derived from the previous days light attenuation profiles. All glassware used for the manipulation of seawater was cleaned with 10 % HCL (reagent grade, 37 %) between CTD sampling iterations and rinsed thoroughly with Milli-Q high purity water within sampling iterations. Chemicals and solvents were analytical and High Performance Liquid Chromatography (HPLC) grade respectively, supplied by Sigma-Aldrich (UK) unless otherwise stated. Stable isotope salts ($^{15}NH_4Cl$, $Na^{15}NO_3$, $Na^{15}NO_2$) were supplied by CK gas products Ltd (UK).

A 20 L volume of seawater from each sampling depth was collected in a blacked-out Nalgene container and used for assimilation and regeneration process studies, which

BGD
12, 17781–17816, 2015

ran in parallel, though for differing durations. Seawater used for these incubations was not pre-filtered (i.e. to remove particles greater than a specific size). As an overview, 6 L of this seawater was used for nitrogen assimilation studies while 12 L was used for nitrogen regeneration studies.

NH_4^+ regeneration rate was determined by amending a 4 L volume of seawater in a blacked out container with $^{15}NH_4^+$ at < 10 % of the ambient concentration. This volume was thoroughly mixed and left to stand for 20 min in order to ensure homogeneity. Amended seawater was used to fill a 2.2 L incubation bottle, which was placed in a deck incubator at simulated light and temperature for approximately 8 h. The remaining amended seawater was filtered through GF/F glass fibre filters and triplicate 100 mL volumes were set aside for the determination of pre-incubation NH_4^+ concentration and isotopic enrichment by synthesising indophenol as described below. Following the deck incubation, bottle contents were filtered through GF/F filters and the filtrate was distributed between 3 × 100 mL volumes for the determination of post-incubation NH_4^+ concentration and isotopic enrichment by synthesising indophenol.

An identical procedure was used for NH_4^+ and NO_2^- oxidation incubations in which separate 4 L volumes of seawater were amended with $^{15}NO_2^-$ and $^{15}NO_3^-$ respectively at < 10 % of the ambient concentration. The concentration and isotopic enrichment of NO_2^- was determined by synthesising sudan-1 in sample volumes of 100 mL, as described below. The concentration and isotopic enrichment of NO_3^- was determined by first reducing NO_3^- to NO_2^- using a high capacity cadmium column, and then synthesising sudan-1 in volumes of 25–50 mL varying with ambient concentration.

Indophenol was synthesised in samples by adding the first reagent (4.7 g phenol and 0.32 g sodium nitroprusside in 200 mL Milli Q water) in the proportion of 1 mL per 100 mL of sample volume, mixing the sample and leaving for 5 min. The second reagent (1.2 g sodium dichloro-isocyanurate and 2.8 g sodium hydroxide in 200 mL Milli Q) was then added in the proportion of 1 mL per 100 mL sample volume, mixed and left for 8 h at room temperature for indophenol development. Indophenol was collected by solid-phase extraction (SPE). Sudan-1 was synthesised by adding the first reagent (0.8 g

BGD
12, 17781–17816, 2015

of aniline sulphate in 200 mL 3 M HCl) to samples in the proportion 0.5 mL per 100 mL sample volume. Samples were mixed and left for 5 min to homogenise after which sample pH was verified to be ≈ 2.0. Reagent 2 (24 g NaOH and 0.416 g 2-napthol in 200 mL Milli Q) was added in the proportion 0.5 mL per 100 mL sample volume. Samples were again mixed, left for 5 min before sample pH was verified to be approximately 8.0. Sudan-1, the development of which was complete after 30 min of incubation at room temperature, was collected by SPE.

Deuterated internal standards were added to samples immediately prior to SPE collection. Deuterated indophenol and deuterated sudan-1 were synthesised according to methods described previously (Clark et al., 2006, 2007) and purified by HPLC. Standard solutions in methanol were prepared (100 ng μL^{-1}) and the concentration verified against analytical standard solutions (Sigma-Aldrich). Appropriate volumes of deuterated internal standards (i.e. comparable to sample size) were added to samples following acidification by citric acid and prior to SPE collection.

Indophenol and sudan-1 were collected by SPE using 6 mL per 500 mg C18 cartridges (Biotage, UK) which were prepared for sample collection by first rinsing with 5 mL methanol, followed by 5 mL Milli Q water and 5 mL 0.22 µm filtered seawater. Prior to sample collection seawater samples were acidified with 1 M citric acid to a pH of 5.5, before collection by SPE under low vacuum (120 mmHg) at a flow rate of approximately 1 mL min^{-1} without drying. Samples were then rinsed with 5 mL 0.22 µm filtered seawater and 5 mL Milli Q water before being air dried under high vacuum (360 mmHg). Samples were stored frozen until further processing at the land based laboratory.

At the land based laboratory, samples were brought to room temperature and prepared for HPLC purification and Gas Chromatography Mass Spectrometry (GCMS) analysis in the following way. Indophenol samples were eluted from SPE cartridges in 2 mL methanol. Samples were placed in a bench-top centrifuge for 2 min at 20 000 × g to remove particulate material derived from the SPE column. A 500 µL sub-sample was used for HPLC purification and GCMS analysis and the remaining 1.5 mL was stored at −20 °C for any subsequent repetition of the analysis. 500 µL sub-samples were evap-

BGD
12, 17781–17816, 2015

orated under oxygen-free nitrogen (OFN) to 200 µL for HPLC, during which it was essential that samples were not reduced to dryness. 175 µL of the 200 µL samples were purified by HPLC using the preparative system, mobile phases and profile described in Clark et al. (2006) in combination with a Gemini-NX 5u C18 110A 250 × 4.6 mm column (Phenomenex, UK) with sample peak collection at a retention time of 38–40 min. Collected sample fractions were blown dry under OFN at room temperature. Dried samples were stored for > 24 h over anhydrous silica gel at room temperature prior to GCMS analysis. Samples were derivitised in 50 µL of 2.5 % Sylon HT in n-hexane and incubated at 50 °C for 4 h. Samples were analysed by GCMS using the system, ramping profiles and extracted ions described in Clark et al. (2006). Internal standards were used to quantify sample NH_4^+ concentration, and when combined with sample enrichment, the rate of NH_4^+ regeneration was determined by applying the Blackburn–Caperon model (Blackburn, 1979; Caperon et al., 1979).

SPE columns loaded with sudan-1 samples were brought to room temperature and processed for HPLC purification and GCMS analysis in the following way. Sudan-1 samples were eluted from SPE cartridges in 2 mL of ethyl acetate. 100–300 µL sub-samples were used for further processing while the remaining samples were stored at −20 °C and available for subsequent repeated analysis. 100–300 µL sub-samples were blown dry under OFN, re-dissolved in 200 µL methanol and centrifuged in a bench-top unit at 20 000 × g for 2 min to remove particulate material derived from the SPE packing. Samples were transferred to GC vials and purified by HPLC. The HPLC system described in Clark et al. (2007) was used in combination with the Gemini column identified above and the mobile phase profile described in Clark et al. (2014). Sample fractions, which were collected at retention time 25.5–27.5 min, were dried using a Zymark Turbovap evaporation unit at 50 °C using OFN. Dried samples were transferred to GC vials and stored over anhydrous silica gel for 24 h prior to derivitisation in a 50 µL volume of 2.5 % MTBSTFA in ethyl acetate at 70 °C for 2 h. The GCMS unit, ramping profile and extracted ions described in Clark et al. (2007) were used to derive sample NO_2^-/NO_3^- concentration and isotopic enrichment. The rate of NH_4^+ or NO_2^- oxidation

BGD
12, 17781–17816, 2015

was derived by re-arranging the mixing model of Sweeney et al. (1978) as described in Clark et al. (2007) and by applying the Blackburn–Caperon model (Blackburn, 1979; Caperon et al., 1979).

2.2 Nitrogen assimilation measurements and the *f* ratio

Using 6 L of seawater, nitrogen assimilation rates were derived using ^{15}N techniques. Triplicate 660 mL volumes of seawater were separately amended with $^{15}NH_4^+$ and $^{15}NO_3^-$ at an enrichment of < 10 % of the ambient concentration. Bottles were placed in deck incubators in conditions of simulated in-situ light and temperature for an average of 6 h. A volume of un-amended seawater was filtered through GF/F and used to derive the ^{15}N natural abundance in particulate matter. Deck incubations were terminated by filtration onto GF/F filters, which were frozen at −20 °C until isotope ratio mass spectrometry analysis was undertaken at the land based laboratory. The rates of nitrogen assimilation (ρNH_4^+, ρNO_3^-) were determined using the equations of Dugdale and Goering (1967), corrected for nitrogen regeneration using the equations of Kanda et al. (1987).

N-assimilation data (not corrected for isotope dilution) was used to derive *f* ratio values by the original formulation as;

$$f \text{ ratio} = \frac{\rho NO_3^-}{\rho NO_3^- + \rho NH_4^+}$$

The *f* ratio was re-calculated using N-assimilation rate data corrected for isotope dilution (f_c ratio). An additional formulation (f_{regen} ratio) calculated the *f* ratio by including a consideration of previously regenerated NO_3^- within P_1, represented as the fraction of the total NO_3^- pool remaining as new NO_3^- (R_{NO_3});

$$f_{regen} \text{ ratio} = \frac{(\rho NO_3^- \cdot R_{NO_3})}{((\rho NO_3^- \cdot R_{NO_3}) + \rho NH_4^+)}$$

BGD
12, 17781–17816, 2015

The term R_{NO_3} was calculated using the following procedure and assumptions; it was assumed that R_{NO_3} was conserved (i.e. no mixing took place); that NO_3^- assimilation was restricted to a 12 h light phase; that phytoplankton did not differentiate between "new" and "regenerated" NO_3^-; that the measured rate of NO_2^- oxidation (which regenerates NO_3^-) was sustained for each 24 h iteration. As an indication of the utility of using NO_3^- assimilation and regeneration processes to reflect NO_3^- pool turnover, a variance of up to ±25 % in calculated compared to measured NO_3^- pool concentration was measured on a daily basis. However, over the duration of the study (T_{-1}–T_7) this difference was −0.2 %, indicating that changes in ambient NO_3^- concentration were adequately described by considering only these processes within the constraints stated.

Using T_{-1} as an example, the ambient pool was assumed to have a R_{NO_3} value of 1, indicating that it was composed only of "new" NO_3^-. The amount of NO_3^- regenerated in this 24 h period was calculated. The value of R_{NO_3} after this 24 h period was calculated by dividing the ambient pool concentration (all new NO_3^- for this first time point) by the sum of ambient and regenerated NO_3^- to give a value of 0.94. For the next 24 h period (T_0), the concentration of "new" NO_3^- was calculated by multiplying the T_0 ambient NO_3^- concentration by the T_{-1} R_{NO_3} value. The R_{NO_3} value at the end of this 24 h period was calculated by dividing the concentration of new NO_3^- by the sum of ambient and newly regenerated (i.e. within T_0) NO_3^- to provide a value of 0.81. This process was repeated for the study period.

2.3 Primary productivity measurements

Phytoplankton productivity was measured using the ^{14}C method (Tilstone et al., 2009). Samples were collected pre-dawn from 5 depths (97, 55, 33, 14, 1 % sPAR). Triplicate 75 mL subsamples were amended with between 185 and 740 kBq (5–20 µCi) $NaH^{14}CO_3$ and incubated on-deck for 24 h at simulated sPAR depth. Incubations were

BGD
12, 17781–17816, 2015

terminated by sequential filtration through 2 and 0.2 µm polycarbonate filters. ^{14}C disintegration was measured on-board using a TriCarb liquid scintillation counter.

2.4 Chlorophyll concentration

Chlorophyll *a* samples were collected simultaneously with seawater used for primary productivity measurements; 250 mL subsamples were collected from 5 depths (97, 55, 33, 14, 1 % sPAR) from pre-dawn CTD casts and immediately filtered sequentially through a 2 and 0.2 µm polycarbonate filters. Filters were soaked in 10 mL 90 % acetone for 12 h and extracts analysed fluorometrically using a Trilogy Turner fluorometer calibrated against pure chlorophyll *a* standards (Sigma).

2.5 Microscopy

Seawater samples were collected from 5 depths (97, 55, 33, 14, 1 % sPAR) during pre-dawn CTD casts. Samples were immediately fixed in acid-Lugol's iodine solution (2 % final concentration). Where possible cells were identified to species-level according to the published literature and assigned to three functional groups (diatoms (centric & pennate), dinoflagellates, flagellates). Cells were enumerated and expressed as cells mL^{-1}.

2.6 Inorganic nutrients

Seawater samples were collected from a range of depths during pre-dawn CTD casts into cleaned, acid-washed, and "aged" high density polyethylene sample bottles, using clean handling and analysis procedures. Samples were analyzed immediately. Nitrate, nitrite, ammonium, phosphate and silicate were measured colorimetrically with a 5-channel segmented flow Bran and Luebbe AAIII autoanalyzer, using methods described previously (Woodward and Rees, 2001).

BGD
12, 17781–17816, 2015

3 Results and discussion

The inert duel tracers SF_6 and ^3He (Nightingale et al., 2000) in combination with drifter buoys were used in this study so that filament progression and biological community development could be followed in lagrangian mode as the water mass advected offshore (Fig. 1). The loss of tracers to the atmosphere, their dilution due to mixing with unlabelled water and the detection limit of GC analysis constrained patch monitoring duration. A detailed description of filament dynamics forming off Cap Blanc, during this study is presented in Meunier et al. (2012). Both North and South Atlantic Central Water (NACW and SACW respectively) is upwelled in this region and the contribution to filaments from each source can be distinguished; SACW generally contains higher nutrient concentrations and has higher temperature with lower oxygen and salinity. Optimum parameter analysis (Rees et al., 2011) demonstrated that the filament studied was dominated by NACW (50–80 %). P_1 was identified using a combination of near-real time remotely sensed data and water column profiling. Following identification, observational measurements were undertaken and $SF_6/^3He$ tracers were deployed at a depth of 5 m in a square spiral (1.0 km × 0.8 km) around a central drifting buoy. Tracers were detected throughout the upper mixed layer depth of 50 m within 1 day of deployment. Extensive mapping exercises were conducted to describe P_1's progression as the water mass advected offshore in a south-westerly then westerly direction. Mapping enabled the patch centre to be located for daily observational measurements. During this study, P_1 remained tightly constrained for the first 3 days until the patch left the continental shelf area and entered the upper slope and shelf break regions. During this latter stage enhanced vertical mixing due to increased water column depth combined with horizontal sheer associated with patch proximity to the northern edge of the filament lead to P_1 elongation and dispersion. Eight days of lagrangian study was achieved (hereafter referred to as T_0 to T_7; pre-patch observations are referred to as T_{-1}), with one day lost due to challenging weather conditions (T_5, 28 April).

BGD
12, 17781–17816, 2015

3.1 Description of the physical and chemical regime

Selected chemical, biological and physical characteristics of the water column are presented in Figs. 2, 3 and 4. As P_1 advected offshore its temperature increased from ≈ 16.4 °C on T_{-1} to > 17.6 °C by T_7. Profiles of water column temperature demonstrated changes in vertical structure as the mixed layer depth increased from approximately 50 m (T_{-1}–T_2) to 100 m coinciding with the continental shelf to shelf break transition (T_3, Loucaides et al., 2012). Nutrient concentrations in P_1 were greatest during the first day of lagrangian study and then progressively decreased (with the exception of NO_2^-). On average, NO_3^- concentration decreased from 9.0 ± 0.1 to $4.6 \pm 0.3\,\mu mol\,L^{-1}$, Si concentration decreased from 2.7 ± 0.1 to $0.9 \pm 0.1\,\mu mol\,L^{-1}$ and PO_4^{3-} concentration decreased from 0.7 ± 0.1 to $0.4 \pm 0.1\,\mu mol\,L^{-1}$. The greatest decrease in nutrient concentrations occurred on the continental shelf. Following advection over the shelf break, these nutrient concentrations continued to decrease albeit at a lower rate. By contrast, NO_2^- concentration remained relatively stable for the duration of the study at $0.31 \pm 0.05\,\mu mol\,L^{-1}$ while a simple increasing or decrease trend in NH_4^+ concentration was not evident; an average value of $0.8 \pm 0.23\,\mu mol\,L^{-1}$ was measured.

Nutrient stoichiometry of the upwelled P_1 water mass indicated nitrogen deficiency (Fig. 3); regression provided a N : P value of 13.9 : 1 compared to a value of 17.7 : 1 below the mixed layer (incorporating depths up to 1400 m). N : P ratios of 7.2–12.3 were reported in the Benguela upwelling system by Gregor and Monteiro (2013). These authors identified denitrification and sulphate reduction as anoxic benthic processes leading to this deficiency, supported by Flohr et al. (2014) who suggested that the Namibian shelf's mud belt is a region of continuous N loss and P efflux to the pelagic environment. In the Mauritanian upwelling system, interactions between upwelled waters and sub-oxic conditions within the pelagic environment have been suggested in modelling studies (Glessmer et al., 2009) and supported by biogeochemical evidence (Rees et al., 2011). Pelagic nitrification associated with oxygen minimum zones leads to a loss of N from this system in the form of N_2O (Rees et al., 2011) and will have

BGD
12, 17781–17816, 2015

contributed to the relative N-deficiency reported here. An average P_1 phosphate excess (P*) of $72 \pm 18\,\mathrm{nmol\,L^{-1}}$ indicated that P_1 exported phosphate to the adjacent oligotrophic gyre of the North Atlantic. The magnitude of this export was less than the value of $< 300\,\mathrm{nmol\,L^{-1}}$ reported for phosphate advection to the south Atlantic gyre by the Benguela upwelling system (Flohr et al., 2014). A P* decline towards zero would be anticipated with offshore advection in support of N_2 fixation (Deutsch et al., 2007).

Analysis demonstrated that nutrient drawdown during P_1 progression was driven by biological processes (Loucaides et al., 2012); factors such as horizontal and vertical mixing with low nutrient water masses derived from outside of the upwelled filament were unlikely to have made a significant contribution. However, an entrainment event associated with increased mixed layer depth lead to a small but measurable recovery in nutrient concentrations during T_3–T_4.

Nutrient drawdown supported high rates of primary production. Rates were measured within the range 0.1–0.7 $\mathrm{mol\,C\,m^{-2}\,d^{-1}}$ which exceeded that measured in other upwelling areas; values of 0.02–0.21 $\mathrm{mol\,C\,m^{-2}\,d^{-1}}$ were reported for the Iberian upwelling (Joint et al., 2001; Álvarez-Salgado et al., 2002; Arístegui et al., 2006), 0.01–0.46 $\mathrm{mol\,C\,m^{-2}\,d^{-1}}$ were reported for the Peruvian upwelling (Fernández et al., 2009), an average of 0.23 $\mathrm{mol\,C\,m^{-2}\,d^{-1}}$ was reported for the Southern Benguela (Shannon and Field, 1985) and 0.07 $\mathrm{mol\,C\,m^{-2}\,d^{-1}}$ was reported for Californian Upwelling Ecosystems (Santoro et al., 2010). Results demonstrated that on average 80 % of this productivity was associated with the $> 2\,\mu\mathrm{m}$ size fraction.

In terms of distribution, the highest rates of primary productivity were associated with the continental shelf region, with rates decreasing as P_1 advected over the shelf break. This distribution was characteristic of the coastal northwest African region, with high biological productivity associated with the region of continental shelf influenced by upwelling (Mittelstaedt, 1991; Arístegui et al., 2009).

BGD
12, 17781–17816, 2015

3.2 Phytoplankton composition and N-assimilation

Freshly upwelled water is extremely low in chlorophyll content and productivity, and would characteristically contain a NO_3^- concentration in the range 9–15 µmol L^{-1} for this region (Arístegui et al., 2009, noting that P_1's composition of NACW and SACW would place freshly upwelled water towards the upper end of this range). Consequently, productivity had become established and decreased NO_3^- by up to 6 µmol L^{-1} prior to this study which followed the removal of a further 4 µmol L^{-1} of NO_3^-. During P_1 progression, clear transitions in phytoplankton abundance, N-biomass and N-assimilation activity took place (Fig. 5). The highest abundance of all phytoplankton was measured during the first 3 days of lagrangian study (T_0–T_2). Although flagellates were numerically dominant, diatoms dominated carbon biomass (data not shown). Cell abundance decreased beyond T_2 although specific phytoplankton classes represented a consistent proportion of total abundance suggesting that selective removal was not an important factor; for the duration of this study, diatoms represented 12.7 ± 5.7 %, dinoflagellates represented 0.10 ± 0.02 %, flagellates represented 87.2 ± 5.7 % of total cell abundance. The trend of progressively diminishing phytoplankton abundance was reflected in the concentration of PON which decreased by 75 % within 8 days.

During this study, NH_4^+ assimilation was measured within the range 6.1–32.8 nmol L^{-1} h^{-1}, while NO_3^- assimilation was measured within the range 3.9–43.8 nmol L^{-1} h^{-1}. There are relatively few studies of N-assimilation in the NW African region against which to draw comparisons; NO_3^- assimilation measured within the photic zone was reported in the range < 0.2–31 nmol L^{-1} h^{-1} (Varela et al., 2005; Dugdale et al., 1990) while NH_4^+ assimilation was reported in the range < 0.2–1.0 nmol L^{-1} h^{-1} (Varela et al., 2005). The range in NO_3^- assimilation was comparable with previous studies while NH_4^+ assimilation had a more prominent role in P_1 than previously reported. This is perhaps the most striking observation; that rates of NH_4^+ and NO_3^- assimilation were broadly similar, despite the difference in N-source avail-

BGD
12, 17781–17816, 2015

ability. The average P_1 NH_4^+ and NO_3^- concentrations were $0.80 \pm 0.23\,\mu mol\,L^{-1}$ and $6.22 \pm 1.20\,\mu mol\,L^{-1}$ respectively, differing by almost one order of magnitude. Results underscore the importance of regenerated nitrogen in supporting phytoplankton nitrogen requirements even from the early stages of upwelling and imply that this form of inorganic nitrogen was rapidly recycled. The significance of N regeneration in upwelling regions has previously been highlighted for the Iberian, the Northern Benguela and Chilean upwelling systems (Clark et al., 2011; Fernandez and Farías, 2012; Benavides et al., 2014).

Within the conveyor belt scheme describing productivity cycles in upwelling systems (Wilkerson and Dugdale, 2008), the increase of phytoplankton growth in response to favourable light and nutrient conditions (shift-up phase) is followed by a shift-down phase driven by factors such as sedimentation and grazing. Cycles last between five and seven days. The trend of progressively diminishing indicators of phytoplankton abundance and activity in combination with a calculated residence time within the photic zone of 3 days for upwelled water prior to T_0 (Meunier et al., 2012; Loucaides et al., 2012) suggested that the peak and shift-down stages of phytoplankton productivity were investigated here. Contributory factors (excluding sedimentation and grazing for which we have no data) to the shift-down phase are discussed below.

In previous studies of upwelling regimes, inorganic nutrient availability has been identified as a limiting resource driving changes in community structure and productivity (Wilkerson and Dugdale, 2008). Nutrient limitation of larger cells, which dominated productivity in the present study, may have been a contributory factor. For example, the average N : Si ratio for the duration of P_1 (4.49 ± 0.78) indicated potential silicate limitation of diatom growth (Brzezinski, 1985; Gilpin et al., 2004). However, relatively high nutrient concentrations were detected by the studies end and a shift in community structure was not observed; the comparable decrease in cell abundance across all phytoplankton classes implied a less specific driver behind the decrease in biomass during the relatively short duration of this study.

BGD
12, 17781–17816, 2015

Light may be considered as a limiting resource; profiles of light intensity and optical depth diminish during the prolific growth of phytoplankton in surface waters; average daily light exposure for cells will also diminish during water column structure transitions as observed beyond T_2 where MLD exceeded the 1 % sPAR depth. Under these circumstances, light limitation would be expressed as a preferential use of NH_4^+ over NO_3^- due to the differential energetic demands (Clark et al., 2002; Flynn et al., 2002). This was not observed during T_{-1}–T_2. However, NH_4^+ assimilation rate consistently exceeded NO_3^- assimilation beyond T_3 (the point at which MLD exceeded the 1 % sPAR depth), potentially supporting this mechanism to describe a characteristic feature of N-assimilation by phytoplankton in upwelled water (Dickson and Wheeler, 1995; Kudela et al., 1997) and contributing to the progressive decrease in indicators of phytoplankton activity and biomass.

3.3 The regeneration of inorganic nitrogen

Evidence presented here has demonstrated that the regeneration of inorganic nitrogen sustained phytoplankton productivity during P_1 development. Nutrient regeneration is a product of heterotrophic DOM degradation by microplankton (bacteria, flagellates, ciliates), following its release from phytoplankton due to grazing or lysis. Alternative routes of NH_4^+ regeneration in upwelling systems such as the activity of zooplankton may represent a minor contribution (Bode et al., 2004; Bronk and Steinberg, 2008; Fernández-Urruzola et al., 2014). During the present study, NH_4^+ was regenerated at rates within the range 9.4–85.0 $\mathrm{nmol\,L^{-1}\,h^{-1}}$ (Fig. 6). We are unaware of previous studies for the Mauritanian system with which to compare this data. For the Benguela system Probyn (1987, 1990) reported comparable rates within the range 0–125 $\mathrm{nmol\,L^{-1}\,h^{-1}}$ while Benavides et al. (2014) reported rates in the range 90–130 $\mathrm{nmol\,L^{-1}\,h^{-1}}$. For the less productive Iberian upwelling system rates of 0.09–2.52 $\mathrm{nmol\,L^{-1}\,h^{-1}}$ have been reported (Clark et al., 2011). The highest rate of NH_4^+ regeneration was measured at T_0, coinciding with the highest ambient ammonium concentration, elevated phytoplankton

BGD
12, 17781–17816, 2015

abundance and productivity although a clear trend during P_1 progression was not apparent given the limited data available (specifically the lack of data for T_{5-7}; T_5 due to challenging weather conditions and T_{6-7} due to sample loss). An NH_4^+ pool turnover of $1.2 \pm 0.7\,d^{-1}$ due to regeneration and a ratio of 1.7 ± 1.1 for NH_4^+ regeneration to assimilation rate demonstrated the rapidity of NH_4^+ recycling that was sufficient to meet phytoplankton requirements.

An additional sink for regenerated NH_4^+ is the nitrification process. The sequential oxidation of NH_4^+ to NO_2^- and NO_3^- is known not to be restricted to aphotic depths (Clark et al., 2008, 2014) and has been reported in other upwelling systems (Clark et al., 2011; Fernandez and Farías, 2012; Benavides et al., 2014). On average, 20 ± 10 % of regenerated NH_4^+ entered the nitrification pathway. Rates of NH_4^+ and NO_2^- oxidation were 0.30–8.75 and 25.55–81.11 $nmol\,L^{-1}\,h^{-1}$ respectively, resulting in an average turnover of 0.3 ± 0.2 and $0.2 \pm 0.1\,d^{-1}$ for NO_2^- and NO_3^- respectively. We are unaware of previous nitrification rate measurements for the Mauritanian system and as a general observation such measurements are rare for upwelling systems. For the Benguela system, NO_3^- regeneration rates of 0.6–15.5 $nmol\,L^{-1}\,h^{-1}$ have been reported (Füssel et al., 2011; Benavides et al., 2014). In the Iberian system, Clark et al. (2011) reported rates of 0.06–3.74 and 0.04–24.76 $nmol\,L^{-1}\,h^{-1}$ for NH_4^+ and NO_2^- oxidation respectively.

The average coupling ratio (NH_4^+ : NO_2^- oxidation rate) was 0.11 ± 0.07, indicating that these processes were substantively uncoupled; NO_2^- oxidation rate exceeded NH_4^+ oxidation rate by several fold as previously reported (Lipschultz et al., 1990; Beman et al., 2010, 2013; Clark et al., 2011, 2014; Füssel et al., 2011; Fernandez and Farías, 2012). The extent of decoupling would imply that NO_2^- oxidation was unsustainable, as NO_2^- would be removed within 1 day at the prevailing NO_2^- oxidation rates. However, a NO_2^- concentration of $\approx 0.3\,\mu mol\,L^{-1}$ persisted in the photic zone for the duration of the study indicating an approximate balance between NO_2^- production and consumption processes. Füssel et al. (2011) suggested that in suboxic environments NO_2^- produced

BGD
12, 17781–17816, 2015

via NO_3^- reduction (the first stage of denitrification) could, in combination with NH_4^+ oxidation, support the observed rates of NO_2^- oxidation. For the present study pelagic oxygen concentrations exceeded 200 µmnol L^{-1} (results not shown) suggesting that denitrification was unlikely to be a significant NO_2^- source. These observations could however be reconciled by a mechanism in which particle bound nitrifying organisms existed in close physical and chemical association. Though not demonstrated in upwelling systems, diverse sources of evidence support this association (Ward, 2008). Via this mechanism the microbially mediated degradation of particulate organic matter would regenerate NH_4^+ directly supporting NH_4^+ oxidation; resultant NO_2^- would support NO_2^- oxidation and regenerated NO_3^- would be released from particles. In contrast, neither NH_4^+ nor NO_2^- would be released from particles to an extent that reflected the stoichiometric rate relationships (potentially contributing to the persistent budgetary "NH_4^+ deficit" previously identified in the Iberian upwelling study of Clark et al., 2011). If such a mechanism were to operate, specific tracer methods would underestimate N-regeneration rates (specifically NH_4^+ regeneration and oxidation rates) in ecosystems characteristically enriched in newly formed marine particles. If this were the case, the extent of decoupling would imply that the substantial majority of nitrification within P_1 was associated with particles. It is unlikely that the micro-environment of marine particles reflects that of bulk water, offering a rationale for our inability to establish robust relationships between environmental factors and nitrification rates beyond light inhibition, which has limited model development (Bouskill et al., 2011; Füssel et al., 2011; Smith et al., 2014a). Additionally, should such a mechanism operate, particle bound nitrifying organisms would be alleviated to an extent from direct competition with phytoplankton for NH_4^+ (Smith et al., 2014b).

3.4 *F* ratio formulations

The present study demonstrated that nitrification was measurable from the inception of P_1 implying that the fraction of regenerated NO_3^- progressively increased within days

BGD
12, 17781–17816, 2015

of freshly upwelled water reaching the photic zone. f ratio formulations for P_1 are presented in Fig. 7 using simultaneously measured rates of N-assimilation and regeneration. Using the original formulation, the highest f ratio values were derived during the first 3 days of lagrangian study, generally decreasing as P_1 advected offshore. Correcting f ratio values for isotope dilution (f_c ratio) made only minor differences. However, accounting for the fraction of regenerated NO_3^- (in addition to isotope dilution; f_{regen} ratio) lead to a cumulative decrease in values relative to the original formulation. Results implied that within ≈ 6 days, the fraction of regenerated NO_3^- was greater than 50 % and that the transition from "new" to a "regenerated" NO_3^- pool occurred rapidly (i.e. the order of days, not weeks). Given the evidence for nitrification in other upwelling systems (Ward, 2005; Fernández et al., 2009; Clark et al., 2011; Benavides et al., 2014), it is likely that NO_3^- based exportable production from such systems has been over-estimated historically.

3.5 Calculating the carbon export of P_1

Carbon export supported by new production was estimated using the approach of Eppley and Peterson (1979) as the product of f ratio and primary production. We compared the original formulation (f ratio) to alternative formulations; f_c ratios (corrected for isotope dilution) and f_{regen} ratio (corrected for isotope dilution and regenerated NO_3^-).

Rees et al. (2011) estimated that the time taken for P_1 to mature from newly-upwelled to open ocean conditions was approximately 14 days, which we confirmed by extrapolation of integrated primary production rates along an exponential gradient ($PP = 801.72e^{-0.253\,Time}$, $r^2 = 0.93$). Rates decreased from 0.69 mol C m^{-2} d^{-1} (T_{-1}) to approximately 0.02 mol C m^{-2} d^{-1} on day 14, comparable to rates reported for the oligotrophic north east Atlantic (Tilstone et al., 2009). The mean area of P_1 was estimated from surface sea temperature images at 1.29×10^4 km^2 while upwelling activity characteristics were also considered. For the purpose of this estimation we assumed that the persistence of upwelling north of 20° N enabled extrapolation of primary produc-

BGD
12, 17781–17816, 2015

tion measured during P_1 over 12 months. By integrating primary production over the 14 day period between maximum upwelling and open-ocean conditions and extrapolating to the mean filament area we estimated annual primary production of 12.38 Tg C. The fraction of annual productivity available for export derived using the *f* ratio was 6.19 Tg C (50 %); using the f_c ratio was 6.01 Tg C (49 %); using the f_{regen} ratio was 4.73 Tg C (38 %). Comparisons with previous estimations are complicated by differences in filament location, geographical area, activity, and integration depth, ranging from 1.12–2.62 Tg C y^{-1} (Helmke et al., 2005) to 3.1 Tg C y^{-1} (Álvarez-Salgado et al., 2007), which are of similar order to our f_{regen} ratio estimates. Within the constraints of our assumptions, results suggest that both isotope dilution and the fraction of previously regenerated NO_3^- can be important sources of error for N-based estimations of C-export.

4 Conclusions

For open ocean systems, the limitation to the new production paradigm that NO_3^- is not necessarily "new" is now well established; to this we add that even within upwelling regions where genuinely new NO_3^- is supplied to the photic zone, the fraction of regenerated NO_3^- increases rapidly. Since the instantaneous ratio of new to regenerated NO_3^- cannot readily be derived this adds uncertainty to *f* ratio values. Upwelling zones are unquestionably highly productive. However, our data indicate that nitrification in these waters is significant and impacts upon *f* ratio derived estimations of new production and carbon export.

Acknowledgements. We thank Carol Robinson (chief scientist), Ricardo Torres and Phil Nightingale for cruise leadership and SF_6 mapping, and the officers and crew of the RRS Discovery cruise D338. We also thank Lisa Al-Moosawi for isotope ratio mass-spectrometry analysis. This study was supported by NERC grant NE/C517176/1 (UK-SOLAS) and by Theme 2 of NERC Oceans 2025.

BGD
12, 17781–17816, 2015

References

Álvarez-Salgado, X. A., Beloso, S., Joint, I., Nogueira, E., Chou, L., Perez, F. F., Groom, S., Cabanas, J. M., Rees, A. P., and Elskens, M.: New production of the NW Iberian shelf during the upwelling season over the period 1982–1999, Deep-Sea Res. Pt. I, 49, 1725–1739, doi:10.1016/S0967-0637(02)00094-8, 2002.

Álvarez-Salgado, X. A., Arístegui, J., Barton, E. D., and Hansell, D. A.: Contribution of upwelling filaments to offshore carbon export in the subtropical Northeast Atlantic Ocean, Limnol. Oceanogr., 52, 1287–1292, doi:10.4319/lo.2007.52.3.12872007, 2007.

Arístegui, J., Álvarez-Salgado, X. A., Barton, E. D., Figueiras, F. G., Hernández-León, S., Roy, C., and Santos, A. M. P.: Oceanography and fisheries of the Canary Current Iberian region of the Eastern North Atlantic, in: The global coastal ocean: Interdisciplinary regional studies and syntheses, edited by: Robinson, A., and Bronk, K. H., Harvard University Press, Cambridge, USA, 877–931, 2006.

Arístegui, J., Barton, E. D., Álvarez-Salgado, X. A., Santos, M. P., Figueiras, F. G., Kifani, S., Hernández-León, S., Mason, E., Machú, E., and Demarcq, H.: Sub-regional ecosystem variability in the Canary Current upwelling, Prog. Oceanogr., 83, 33–43, 2009, doi:10.1016/j.pocean.2009.07.031, 2009.

Beman, J. M., Sachdeva, R., and Fuhrman, J. A.: Population ecology of nitrifying Archaea and bacteria in the Southern California Bight, Environ. Microbiol., 12, 1282–1292, doi:10.1111/j.1462-2920.2010.02172.x, 2010.

Beman, J. M., Shih, J. L., and Popp, B. N.: Nitrite oxidation in the upper water column and oxygen minimum zone of the eastern tropical North Pacific Ocean, Int. Soc. Micro. Ecol., 7, 2192–2205, doi:10.1038/ismej.2013.96, 2013.

Benavides, M., Santana-Falcón Y., Wasmund, N., and Arístegui, J.: Microbial uptake and regeneration of inorganic nitrogen off the coastal Namibian upwelling system, J. Marine Syst., 140, 123–129, doi:10.1016/j.jmarsys.2014.05.002, 2014.

Blackburn, T. H.: Method for measuring rates of NH_4^+ turnover in anoxic marine sediments, using $^{15}N\text{-}NH_4^+$ dilution technique, Appl. Environ. Microb., 37, 760–765, 1979.

Bronk, D. A. and Steinberg, D. K.: Nitrogen Regeneration, in: Nitrogen in the Marine Environment, edited by: Capone, D., Bronk, D. A., Mulholland, M. R., and Carpenter, E. J., Elsevier Press, London, UK, 385–467, 2008.

BGD
12, 17781–17816, 2015

Brzezinski, M. A.: The Si-C-N ratio of marine diatoms – interspecific variability and the effect of some environmental variables, J. Phycol., 21, 347–357, doi:10.1111/j.0022-3646.1985.00347.x, 1985.

Bode, A., Barquero, S., Gonzalez, N., Alvarez-Ossorio, M. T., and Varela, M.: Contribution of heterotrophic plankton to nitrogen regeneration in the upwelling ecosystem of A Coruña (NW Spain), J. Plankton Res., 26, 11–28, doi:10.1093/plankt/fbh003, 2004.

Bouskill, N. J., Eveillard, D., Chien, D., Jayakumar, A., and Ward, B. B.: Environmental factors determining ammonia-oxidizing organism distribution and diversity in marine environments, Environ. Microbiol, 14, 714–729, doi:10.1111/j.1462-2920.2011.02623.x, 2011.

Caperon, J., Schell, D., Hirota, J., and Laws, E.: Ammonium excretion rates in Kaneohe Bay, Hawaii, measured by a ^{15}N isotope dilution technique, Mar. Biol., 54, 33–40, doi:10.1007/BF00387049, 1979.

Chavez, F. and Messié, M.: A comparison of Eastern Boundary Upwelling Ecosystems, Prog. Oceanogr., 83, 80–96, doi:10.1016/jpocean.2009.07.32, 2009.

Clark, D. R., Flynn, K. J., and Owens, N. J. P.: The large capacity for dark nitrate-assimilation in diatoms may overcome nitrate limitation of growth, New Phytol., doi:10.1046/j.1469-8137.2002.00435.x, 155, 101–108, 2002.

Clark, D. R., Fileman, T. W., and Joint, I.: Determination of ammonium regeneration rates in the oligotrophic ocean by gas chromatography/mass spectrometry, Mar. Chem., 98, 121–130, doi:10.1016/j.marchem.2005.08.006, 2006.

Clark, D. R., Rees, A. P., and Joint, I.: A method for the determination of nitrification rates in oligotrophic marine seawater by gas chromatography/mass spectrometry, Mar. Chem., 103, 84–96, doi:10.1016/j.marchem.2006.06.005, 2007.

Clark, D. R., Rees, A. P., and Joint, I.: Ammonium regeneration and nitrification rates in the oligotrophic Atlantic Ocean: implications for new production estimates, Limnol. Oceanogr., 53, 52–62, doi:10.4319/lo.2008.53.1.0052, 2008.

Clark, D. R., Miller, P. I., Woodward, E. M. S., and Rees, A. P.: Inorganic nitrogen assimilation and regeneration in the coastal upwelling region of the Iberian Peninsula, Limnol. Oceanogr., 56, 1689–1702, doi:10.4319/lo.2011.56.5.1689, 2011.

Clark, D. R., Brown, I. J., Rees, A. P., Somerfield, P. J., and Miller, P. I.: The influence of ocean acidification on nitrogen regeneration and nitrous oxide production in the northwest European shelf sea, Biogeosciences, 11, 4985–5005, doi:10.5194/bg-11-4985-2014, 2014.

BGD
12, 17781–17816, 2015

D'Asaro, E. A.: Lagrangian trajectories on the Oregon shelf during upwelling, Cont. Shelf Res., 24, 1421–1436, doi:10.1016/j.csr.2004.06.003, 2004.
Dickson, M. L. and Wheeler, P. A.: Nitrate uptake rates in a coastal upwelling regime – A comparison of PN-specific, absolute and chl a-specific rates, Limnol. Oceanogr., 40, 533–543, doi:10.4319/lo.1995.40.3.0533, 1995.
Deutsch, C., Sarmiento, J. L., Sigman, D. M., Gruber, N., and Dunne, J. P.: Spatial coupling of nitrogen inputs and losses in the ocean, Nature, 445, 163–167, doi:10.1038/nature05392, 2007.
Dugdale, R. C. and Goering, J. J.: Uptake of new and regenerated forms of nitrogen in primary productivity, Limnol. Oceanogr., 12, 196–206, doi:10.4319/lo.1967.12.2.0196, 1967.
Dugdale, R. C., Wilkerson, F. P., and Morel, A.: Realization of new production in coastal upwelling areas: a means to compare relative performance, Limnol. Oceanogr., 35, 822–829, doi:10.4319/lo.1990.35.4.0822, 1990.
Eppley, R. W. and Peterson, B. J.: Particulate organic matter flux and planktonic new production in the deep ocean, Nature, 282, 677–680, doi:10.1038/282677a0, 1979.
Fernandez, C. and Farías, L.: Assimilation and regeneration of inorganic nitrogen in a coastal upwelling system: ammonium and nitrate utilisation, Mar. Ecol.-Prog. Ser., 451, 1–14, doi:10.3354/meps09683, 2012.
Fernández, C., Raimbault, P., Garcia, N., and Rimmelin, P.: An estimation of annual new production and carbon fluxes in the northeast Atlantic Ocean during, 2001, J. Geophys. Res., 110, C07S13, doi:10.1029/2004JC002616, 2005.
Fernández, C., Farías, L., and Alcaman, M. E.: Primary production and nitrogen regeneration processes in surface waters of the Peruvian upwelling system, Prog. Oceanogr., 83, 159–168, doi:10.1016/j.pocean.2009.07.010, 2009.
Fernández, I. C. and Raimbault, P.: Nitrogen regeneration in the NE Atlantic Ocean and its impact on seasonal new, regenerated and export production, Mar. Ecol.-Prog. Ser., 337, 79–92, doi:10.3354/meps337079, 2007.
Fernández-Urruzola, I., Osma, N., Packard, T. T., Gómez, M., and Postel, L.: Distribution of zooplankton biomass and potential metabolic activities across the northern Benguela upwelling system, J. Marine Syst., 140, 138–149, doi:10.1016/j.jmarsys.2014.05.009, 2014.
Flohr, A., van der Plas, A. K., Emeis, K.-C., Mohrholz, V., and Rixen, T.: Spatio-temporal patterns of C: N: P ratios in the northern Benguela upwelling system, Biogeosciences, 11, 885–897, doi:10.5194/bg-11-885-2014, 2014.

BGD
12, 17781–17816, 2015

Flynn, K. J., Clark, D. R., and Owens, N. J. P.: Modelling suggests that optimization of dark nitrogen-assimilation need not be a critical selective feature in phytoplankton, New Phytol., 155, 109–119, doi:10.1046/j.1469-8137.2002.00436.x, 2002.

Füssel, J., Lam, P., Lavik, G., Jensen, M. M., Holtappels, M., Günter, M., and Kuypers, M. M. M.: Nitrite oxidation in the Namibian oxygen minimum zone, ISME J., 1–10, doi:10.1038/ismej.2011.178, 2011.

Gilpin, L. C., Davidson, K., and Robertsb, E.: The influence of changes in nitrogen: silicon ratios on diatom growth dynamics, J. Sea Res., 51, 21–35, doi:10.1016/j.seares.2003.05.005, 2004.

Glessmer, M., Eden, C., and Oschlies, A.: Contribution of oxygen minimum zone waters to the coastal upwelling off Mauritania, Prog. Oceanogr., 83, 143–150, doi:10.1016/j.pocean.2009.07.015, 2009.

Glibert, P. M., Lipshultz, F., McCarthy, J. J., and Altabet, M. A.: Isotope dilution models of uptake and remineralization of ammonium by marine plankton, Limnol. Oceanogr., 27, 639–650, doi:10.4319/lo.1982.27.4.0639, 1982.

Gregor, L. and Monteiro, P. M. S.: Seasonal cycle of N : P:TA stoichiometry as a modulator of CO_2 buffering in eastern boundary upwelling systems, Geophys. Res. Lett., 40, 5429–5434, doi:10.1002/2013GL058036, 2013.

Helmke, P., O. Romero, and Fischer, G.: Northwest African upwelling and its effect on offshore organic carbon export to the deep sea, Global Biogeochem. Cy., 19, GB4015, doi:10.1029/2004GB002265, 2005.

Intergovernmental Oceanographic Commission, Paris (France): Protocols for the Joint Global Flux Study (JGOFS) core measurements, Manuals Guides, 29, 1994.

Joint, I., Rees, A. P., and Woodward, E. M. S.: Primary production and nutrient assimilation in the Iberian upwelling in August 1998, Prog. Oceanogr., 51, 303–320, doi:10.1016/S0079-6611(01)00072-6, 2001.

Joint, I., Inall, M., Torres, R., Figueiras, F. G., Álvarez-Salgado, X. A., Rees, A. P., and Woodward, E. M. S.: Two Lagrangian experiments in the Iberian Upwelling System: tracking an upwelling event and an offshore filament, Prog. Oceanogr., 51, 221–248, doi:10.1016/S0079-6611(01)00068-4, 2001.

Kanda, J., Laws, E. A., Saino, S. T., and Hattori, A.: An evaluation of isotope dilution effect from conventional data sets of ^{15}N uptake experiments, J. Plankton Res., 19, 79–90, doi:10.1093/plankt/9.1.79, 1987.

BGD
12, 17781–17816, 2015

Kudela, R. M., Cochlan, W. P., and Dugdale, R. C.: Carbon and nitrogen uptake response to light by phytoplankton during an upwelling event, J. Plankton Res., 19, 609–630, doi:10.1093/plankt/19.5.609, 1997.

Loucaides, S., Tyrrell, T., Achterberg, E. P., Torres, R., Nightingale, P. D., Kitidis, V., Serret, P., Woodward, M., and Robinson, C.: Biological and physical forcing of carbonate chemistry in an upwelling filament off northwest Africa: results from a Lagrangian study, Global Biogeochem. Cy., 26, GB3008, doi:10.1029/2011GB004216, 2012.

Lipshultz, F., Wofsy, S. C., Ward, B. B., Codispoti, L. A., Freidrich, G., and Elkins, J. W.: Bacterial transformations of inorganic nitrogen in the oxygen deficient waters of the Eastern Tropical South Pacific Ocean, Deep-Sea Res., 37, 1513–1541, 1990.

Martin, A. P. and Pondaven, P.: New production and nitrification in the western subtropical North Atlantic: a modelling study, Global Biogeochem. Cy., 20, GB4014, doi:10.1029/2005GB002608, 2006.

Meunier, T., Barton, E, D., Barreiro, B., and Torres, R.: Upwelling filaments off Cap Blanc: interaction of the NW African upwelling current and the Cape Verde frontal zone eddy field?, J. Geophys. Res., 117, C08031, doi:1029/2012JC007905, 2012.

Mittelstaedt, E.: The ocean boundary along the northwest African coast: Circulation and oceanographic properties at the sea surface, Prog. Oceanogr., 26, 307–355, doi:10.1016/0079-6611(91)90011-A, 1991.

Nightingale, P. D., Malin, G., Law, C. S., Watson, A. J., Liss, P. S., Liddicoat, M. I., Boutin, J., and Upstill-Goddard, R. C.: In situ evaluation of air–sea gas exchange parameterizations using novel conservative and volatile tracers, Global Biogeochem. Cy., 14, 373–387, doi:10.1029/1999GB900091, 2000.

Pauly, D. and Christensen, V.: Primary production required to sustain global fisheries, Nature, 374, 255–257, doi:10.1038/374255a0, 1995.

Postel, L., Mohrholz, V., and Packard, T. T.: Upwelling and successive ecosystem response in the Northern Benguela Region – an in situ experiment, J. Marine Syst., 140, 73–81, doi:10.1016/j.jmarsys.2014.07.014, 2014.

Probyn, T. A.: Ammonium regeneration by microplankton in an upwelling environment, Mar. Ecol.-Prog. Ser., 37, 53–64, 1987.

Probyn, T. A.: Size-fractionated measurements of nitrogen uptake in aged upwelled waters: implications for pelagic food webs, Limnol. Oceanogr., 35, 202–210, doi:10.4319/lo.1990.35.1.0202, 1990.

BGD
12, 17781–17816, 2015

Rees, A. P., Brown, I. J., Clark, D. R., and Torres, R.: The Lagrangian progression of nitrous oxide within filaments formed in the Mauritanian upwelling, Geophys. Res. Lett., 38, L21606, doi:10.1029/2011GL049322, 2011.
Santoro, A. E., Casciotti, K. L., and Francis, C. A.: Activity, abundance and diversity of nitrifying archaea and bacteria in the central California Current, Environ. Microbiol., 12, 1989–2006, doi:10.1111/j.1462-2920.2010.02205.x, 2010.
Shannon, L. V. and Field, J. G.: Are fish stocks food limited in the southern Benguela pelagic ecosystem?, Mar. Ecol.-Prog. Ser., 22, 7–19, doi:10.3354/meps022007, 1985.
Smith, J. M., Casciotti, K. L., Chavez, F. P., and Francis, C. A.: Differential contribution of archaeal ammonia oxidizer ecotypes to nitrification in coastal surface waters, ISME J., 8, 1704–1714, doi:10.1038/ismej.2014.11, 2014a.
Smith, K. M., Chavez, F. P., and Francis, C. A.: Ammonium uptake by phytoplankton regulates nitrification in the sunlit ocean. PLoS ONE, 9, e108173, doi:10.1371/journal.pone.0108173, 2014b.
Sweeney, R. E., Liu, K. K., and Kaplan, I. R.: Oceanic nitrogen isotopes and their uses in determining the source of sedimentary nitrogen, N. Z. Depart. Sci. Ind. Res. Bull., 220, 9–26, 1978.
Tilstone, G., Smyth, T., Poulton, A., and Hutson, R.: Measured and remotely sensed estimates of primary production in the Atlantic Ocean from 1998 to 2005, Deep-Sea Res. Pt. II, 56, 918–930, doi:10.1016/j.dsr2.2008.10.034, 2009.
Tomczak, M. and Godfrey, J. S.: Regional Oceanography: an Introduction, second Edn., Daya, Delhi, India, p. 390, 2003.
Varela, M., Bode, A., Fernandez, E., Gonzales, N., Kitidis, V., Varela, M., and Woodward, E. M. S.: Nitrogen uptake and dissolved organic nitrogen release in planktonic communities characterized by phytoplankton size structure in the central North Atlantic, Deep-Sea Res. Pt. I, 52, 1637–1661, doi:10.1016/j.dsr.2005.03.007, 2005.
Ward, B.: Nitrogen in the Marine Environment, in: Nitrogen in the Marine Environment, Capone, D., Bronk, D. A., Mulholland, M. R., and Carpenter, E. J., Elsevier Press, London, UK, 199–261, 2008.
Ward, B. B.: Temporal variability in nitrification rates and related biogeochemical factors in Monterey Bay, California, USA, Mar. Ecol.-Prog. Ser., 292, 97–109, doi:10.3354/meps292097, 2005.

BGD
12, 17781–17816, 2015

Wilkerson, F. P. and Dugdale, R. C.: The use of large shipboard barrels and drifters to study the effects of coastal upwelling on phytoplankton dynamics, Limnol. Oceanogr., 32, 368–382, doi:10.4319/lo.1987.32.2.0368, 1987.

Wilkerson, F. P. and Dugdale, R. C.: Coastal Upwelling, in: Nitrogen in the Marine Environment, Capone, D., Bronk, D. A., Mulholland, M. R., and Carpenter, E. J., Elsevier Press, London, UK, 765–801, 2008.

Woodward, E. M. S. and Rees, A. P.: Nutrient distributions in an anticyclonic eddy in the North East Atlantic Ocean, with reference to nanomolar ammonium concentrations, Deep-Sea Res., 48, 775–794, doi:10.1016/S0967-0645(00)00097-7, 2001.

Yool, A., Martin, A. P., Fernández, C., and Clark, D. R.: The significance of nitrification for oceanic new Production, Nature, 447, 999–1002, doi:10.1038/nature05885, 2007.

BGD
12, 17781–17816, 2015

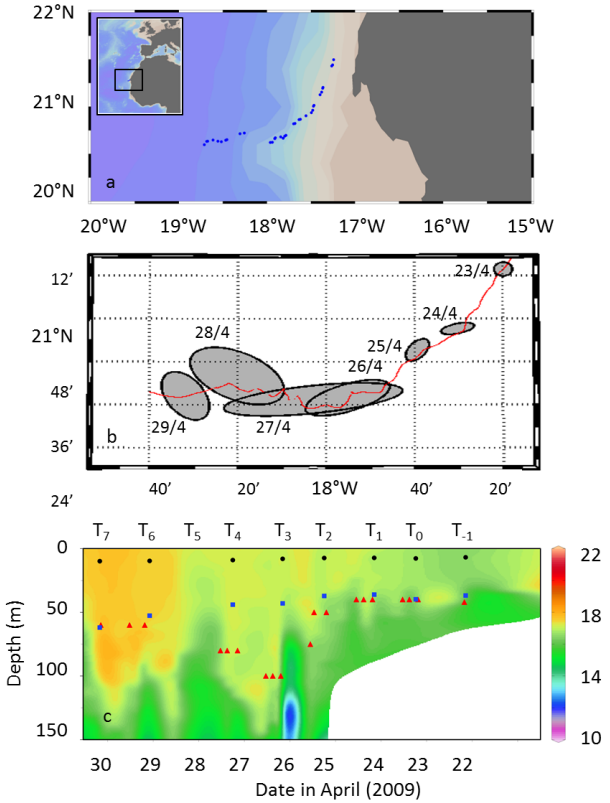

Figure 1. The location of sampling stations is presented in panel **(a)**. Panel **(b)** presents the lateral SF_6 distribution, defined as 40 % of the peak concentration. The red line indicates the track of a central marker buoy used in combination with SF_6 analysis. Panel **(c)** presents water column temperature (˚C) and includes sampling depths for 55 % sPAR (black circles) and 1 % sPAR (blue squares). The depth of the upper mixed layer is indicated (red triangles; Loucaides et al., 2012). Note the reversal of dates in panel **(c)** to aid comparisons with panels **(a)** and **(b)**.

BGD
12, 17781–17816, 2015

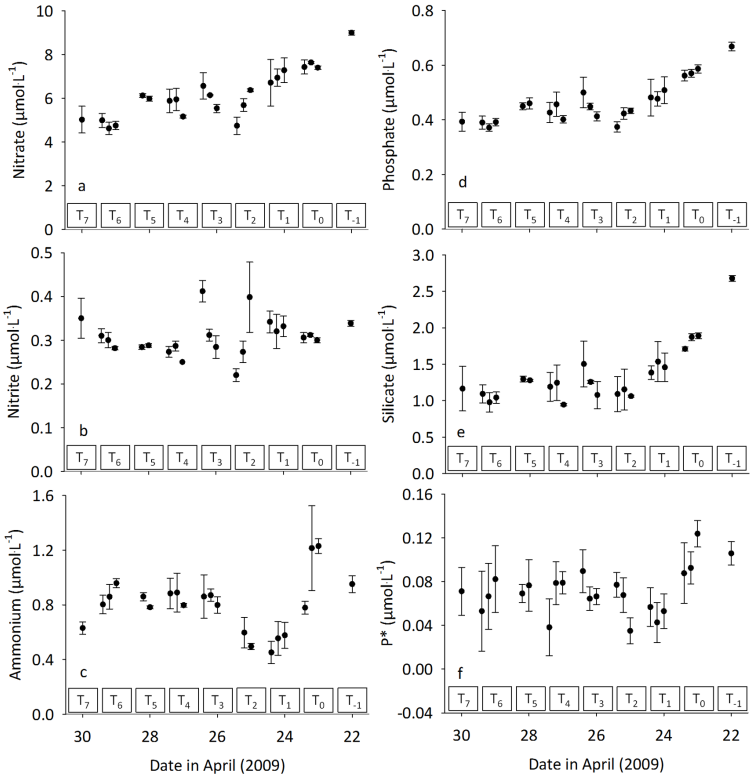

Figure 2. Average concentration of inorganic nutrients within the upper mixed layer; **(a)** nitrate, **(b)** nitrite, **(c)** ammonium, **(d)** phosphate, **(e)** silicate. The phosphate excess (P^*) is presented in panel **(f)**. Note the reversal of dates to aid comparisons between figures.

BGD
12, 17781–17816, 2015

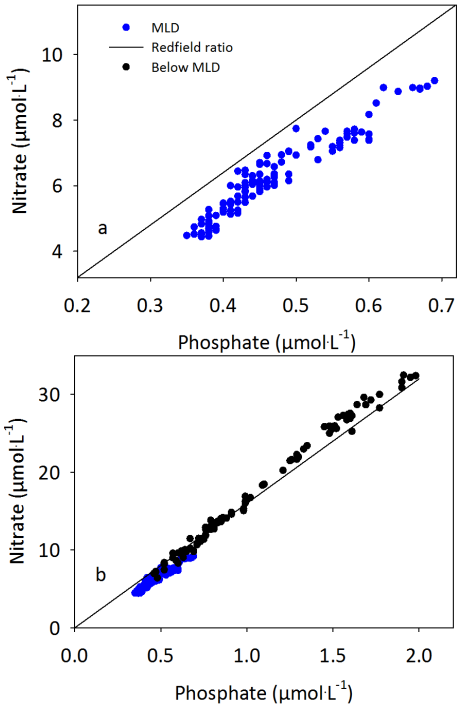

Figure 3. Ratio between ambient concentrations of nitrate and phosphate. The solid regression line is the Redfield ratio of 16 : 1. Data from within the surface mixed layer depth (MLD) are presented in panel **(a)**, the regression of which provides a ratio of 13.9 : 1 and a phosphate excess of 72 ± 18 nmol L^{-1}. Data from below the MLD, presented in panel **(b)** were collected to a maximum depth of 1.4 km. The regression of this data provided a ratio of 17.7 : 1.

BGD
12, 17781–17816, 2015

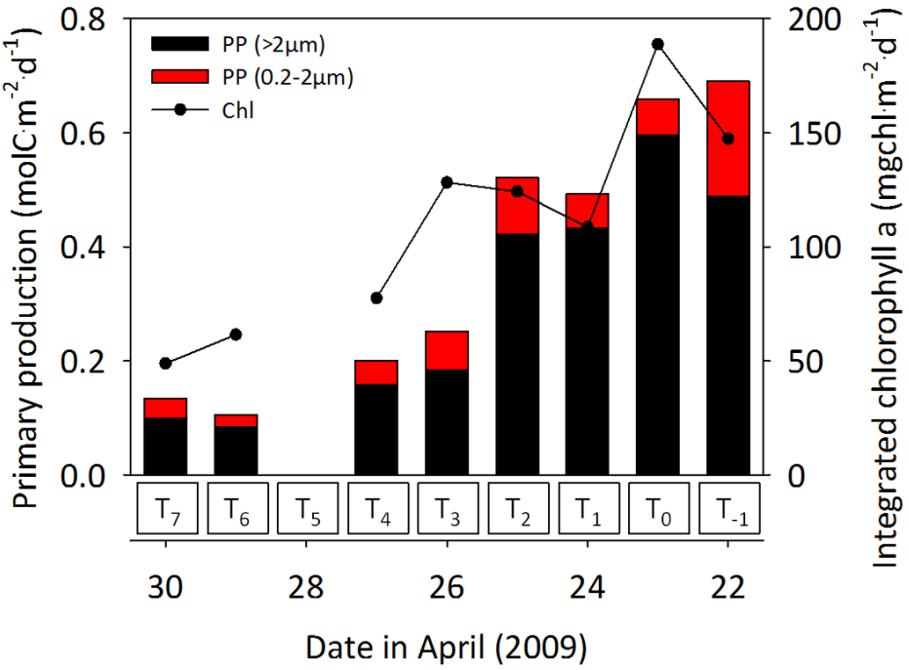

Figure 4. Changes in integrated (photic depth) primary production and integrated chlorophyll concentration in two size fraction (> 2 µm and 0.2–2 µm). Note the reversal of dates to aid comparisons between figures.

BGD
12, 17781–17816, 2015

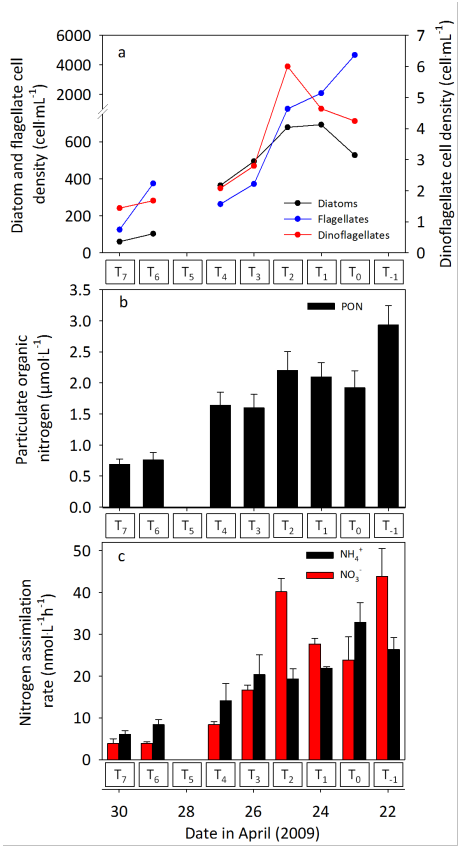

Figure 5. Changes in the abundance of phytoplankton **(a)**, the concentration of particulate organic nitrogen (PON, **(b)**), and the rate of nitrogen assimilation as nitrate and ammonium **(c)**. PON and nitrogen assimilation were measured within the mixed layer at 55 % sPAR. Note the reversal of dates to aid comparisons between figures.

BGD
12, 17781–17816, 2015

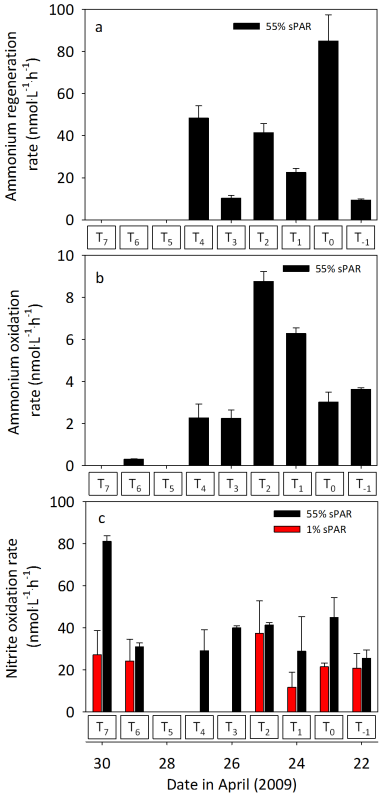

Figure 6. Changes in the rate of ammonium regeneration **(a)**, ammonium oxidation **(b)** and nitrite oxidation **(c)** for samples taken within the mixed layer depth at 55 and 1 % sPAR. Note the reversal of dates to aid comparisons between figures.

BGD
12, 17781–17816, 2015

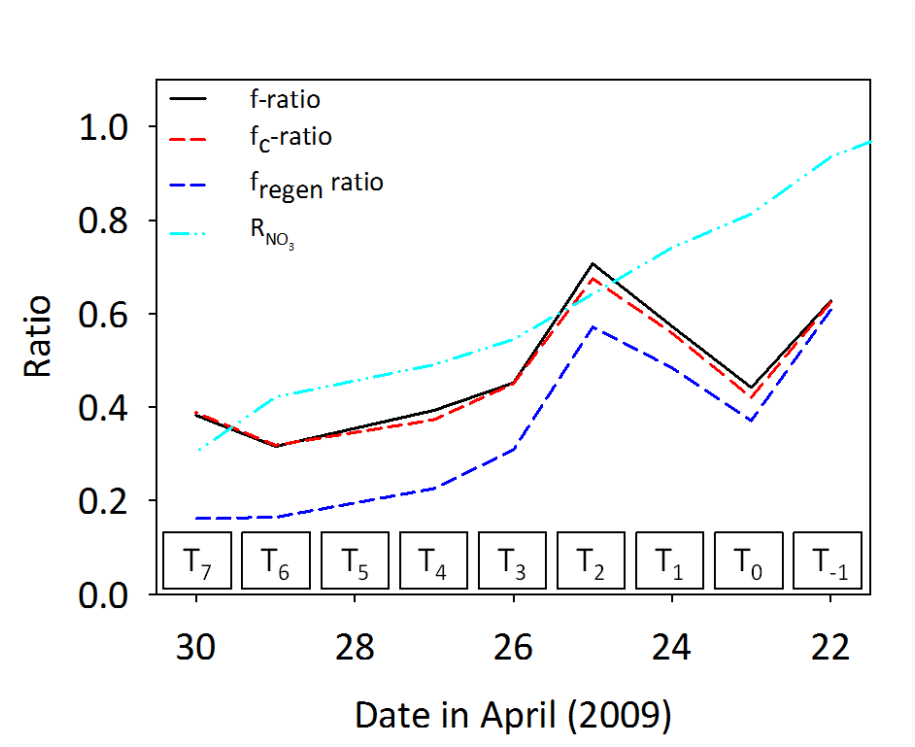

Figure 7. Changes in *f* ratio representations (*f* ratio; f_c ratio corrected for isotope dilution due to nitrogen regeneration; f_{regen}-ratio corrected for isotope dilution and the fraction of the nitrate pool represented by "new" rather than "regenerated" nitrate. The fraction of the nitrate pool represented by "new" nitrate is also presented (R_{NO_3}). Note the reversal of dates to aid comparisons between figures.

BGD
12, 17781–17816, 2015